A high throughput Chromatin ImmunoPrecipitation approach reveals principles of dynamic gene regulation in mammals

Manuel Garber[1,7,*], **Nir Yosef**[1,2,*], **Alon Goren**[1], **Raktima Raychowdhury**[1], **Anne Thielke**[1], **Mitchell Guttman**[1,3], **James Robinson**[1], **Brian Minie**[1], **Nicolas Chevrier**[1], **Zohar Itzhaki**[4], **Ronnie Blecher-Gonen**[4], **Chamutal Bornstein**[4], **Daniela Amann-Zalcenstein**[4], **Assaf Weiner**[5], **Dennis Friedrich**[1], **James Meldrim**[1], **Oren Ram**[1], **Christine Chang**[1,5], **Andreas Gnirke**[1], **Sheila Fisher**[1], **Nir Friedman**[5], **Bang Wong**[1], **Bradley E. Bernstein**[1,6], **Chad Nusbaum**[1], **Nir Hacohen**[1,2], **Aviv Regev**[1,3,6], and **Ido Amit**[1,4,†]

[1]Broad Institute of MIT and Harvard, Cambridge, MA 02142

[2]Harvard Medical School, Boston, MA 02115

[3]Department of Biology, Massachusetts Institute of Technology, Cambridge, MA 02142

[4]Weizmann Institute, Department of Immunology, Rehovot 76100

[5]School of Computer Science and Institute of Life Sciences, Hebrew University, Jerusalem

[6]Howard Hughes Medical Institute

[7]University of Massachusetts Medical School, Bioinformatics and Integrative Biology, Worcester, MA 01605, USA

Abstract

Understanding the principles governing mammalian gene regulation has been hampered by the difficulty in measuring in-vivo binding dynamics of large numbers of transcription factors (TF) to DNA. Here, we develop a high-throughput Chromatin ImmunoPrecipitation (HT-ChIP) method to systematically map protein-DNA interactions. HT-ChIP was applied to define the dynamics of DNA binding by 25 TFs and 4 chromatin marks at 4 time-points following pathogen stimulus of dendritic cells. Analyzing over 180,000 TF-DNA interactions we find that TFs vary substantially in their temporal binding landscapes. This data suggests a model for transcription regulation whereby TF networks are hierarchically organized into cell differentiation factors, factors that bind targets prior to stimulus to prime them for induction, and factors that regulate specific gene programs. Overlaying HT-ChIP data on gene expression dynamics shows that many TF-DNA interactions are established prior to the stimuli, predominantly at immediate-early genes, and identified specific TF ensembles that coordinately regulate gene-induction.

Introduction

The complex gene expression programs that underlie development, differentiation, and environmental responses are primarily determined by binding of sequence-specific transcription factors (TFs) to DNA (Graf and Enver, 2009; Laslo et al., 2006; Struhl, 2001). While it is clear that TFs play a critical role in gene regulation, how these factors work together to control gene expression responses in complex organisms is still not fully understood (Davidson, 2010).

†To whom correspondence should be addressed. ido.amit@weizmann.ac.il.
*These authors contributed equally to this work

To date, systematic efforts to understand the mammalian regulatory code have mostly relied on generalization from studies on simple model organisms (Capaldi et al., 2008; Harbison et al., 2004), *in vitro* experiments, and studies of individual gene loci (Bossard and Zaret, 1998; Cirillo et al., 2002; Thanos and Maniatis, 1992). Genomic approaches, such as correlation analysis of gene expression profiles (Segal et al., 2003), and more recently RNAi perturbation followed by gene expression readouts (Amit et al., 2009), have provided an initial glimpse into the complexity of mammalian gene regulation. However, such approaches cannot distinguish direct from indirect effects and cannot address network redundancy and temporal regulation, thus they provide limited insight into the underlying regulatory mechanisms.

A complementary approach is to measure the temporal *in vivo* binding of TFs to *cis*-regulatory regions under relevant stimuli. Recent advances in genomic technologies allow for unbiased and accurate genome-wide characterization of TF binding using ChIP followed by DNA sequencing (ChIP-Seq) (Barski et al., 2007; Johnson et al., 2007; Mikkelsen et al., 2007). Despite these advances in detection, ChIP remains relatively low throughput (Barski et al., 2007; Gerstein et al., 2010; Johnson et al., 2007; Mikkelsen et al., 2007; Negre et al., 2011; Roy et al., 2010). As a result, little is known about the genome-wide dynamics of protein-DNA interaction networks.

To address these challenges we developed HT-ChIP, a reproducible, high throughput and cost-effective method for ChIP coupled to multiplexed massively parallel sequencing. We used HT-ChIP to investigate the principles of gene regulation in the model system of primary innate immune dendritic cells (DCs) stimulated with the pathogen component lipopolysaccharide (LPS). In response to stimulation, DCs activate a robust, specific, and reproducible response that unfolds over several hours, involves changes of thousands of genes (Amit et al., 2009; Rabani et al., 2011), and plays a critical role in directing the host immune response. We used HT-ChIP to build genome-wide dynamic maps of TF localization to DNA during response of DCs to LPS. We screened antibodies for the most expressed transcription factors and identified ChIP-Seq grade antibodies for 25 TFs, RNA polymerase II (Pol II), and 3 epigenetic modifications. Using these validated antibodies we performed HT-ChIP across four time points upon LPS stimulation. Surprisingly, we find that much of the binding of TFs is pre-coded during differentiation and prior to stimulation, predominantly on immediate early genes. Many of the immediate early genes are associated with High Occupancy Target (HOT) regions similarly to those recently reported in flies and worms (Gerstein et al., 2010; Negre et al., 2011; Roy et al., 2010). By focusing on dynamics of expression and binding, our work further expands the functional role of these HOT regions as potential stimulus dependent induction hubs in mammals.

Our data shows that TFs vary substantially in their binding dynamics, number of binding events, preferred genomic locations and interactions with other TFs. Analysis of these different binding properties together with temporal gene expression and epigenetic marks shows that TFs fall into at least three broad characteristics, suggesting a multilayered architecture. Pioneer TF described recently (Bossard and Zaret, 1998; Cirillo et al., 2002; Ghisletti et al., 2010; Heinz et al., 2010; Lupien et al., 2008) are coded during differentiation, are unchanged in binding location during stimulus and correlate with the cell epigenetic state (Ghisletti et al., 2010; Heinz et al., 2010). A second prominent layer of TF binds thousands of genes in the un-stimulated state and is highly correlated with future stimulus dependent gene induction. A third set of TFs bind dynamically in a stimulus dependent manner and control induction of gene sets enriched for a shared biological activity (e.g. Inflammatory, anti-viral response and cell cycle). Together, our findings demonstrate the importance of global TF dynamic maps in uncovering the principles of the regulatory code. For visual exploration of the data, we developed an extension to the

Integrative Genomics Viewer (IGV (Robinson et al., 2011)), geared specifically towards viewing time course data. The entire data can be viewed from: http://www.weizmann.ac.il/immunology/AmitLab/data-and-method/HT-ChIP.

RESULTS

HT-ChIP: A high-throughput method for mapping in vivo Protein-DNA interactions

We developed HT-ChIP, an automated method for systematic mapping of *in vivo* protein-DNA binding that increases the throughput and sensitivity, while reducing the labor and cost required for ChIP-Seq. Unlike the standard ChIP assay performed in individual tubes, which involves over 25 steps of chromatin washing, reverse crosslinking, DNA purification, gel extraction and library construction (Barski et al., 2007; Johnson et al., 2007; Mikkelsen et al., 2007); HT-ChIP uses magnetic solid phase beads for the immunoprecipitation of protein-DNA complexes, DNA purification, size-selection and library construction eliminating laborious manual processes (Figure 1, Methods). Furthermore, the entire HT-ChIP process is performed in the same well reducing sample loss of precipitated DNA material allowing a significant reduction in the required number of cells (Figure S1A–B, Methods). HT-ChIP further leverages the yield of current next-generation sequencing by multiplexing an arbitrary number of different indexed sequencing adapters, 96 in our case, to combine samples in a single sequencing flow cell (Figure 1A). The data produced by HT-ChIP-Seq is highly correlated with traditional ChIP-Seq data generated both in our labs and by others ((Ghisletti et al., 2010; Heinz et al., 2010); Figure S1C–D).

We used HT-ChIP to reconstruct the dynamic binding network of 25 TFs in primary mouse dendritic cells (DCs) following LPS stimulation (Figure 1C and Table S1). We used RNA-Seq of DC activated with LPS at five time points (0, 1, 2, 4, 6 hours) to identify the most highly expressed TFs in DC (RPKM > 15, totaling 184; see Supplementary Text). We then collected 271 commercially available antibodies targeting these TFs (Figure 1B; Methods). We tested each antibody using a signature readout (Ram et al., 2011) ('ChIP-String') that measures selected genomic DNA regions with high regulatory activity (Ghisletti et al., 2010). We identified 29 antibodies (25 TFs, 3 histone modifications and Pol II) that passed our selection criteria as 'ChIP grade', based on their enrichment on the signature regions and performance in Western blots. These antibodies were then used for HT-ChIP at four time points (0, 0.5, 1, 2 hours) post LPS stimulation, during which most of the transcriptional changes occur (Figure S1F,G).

Comprehensive map of active enhancers and promoters in DC

Recent studies have demonstrated that the ratio between H3K4me3 and H3K4me1 histone marks can be used to identify promoter and enhancer regions (Heintzman and Ren, 2009): promoters are associated with a higher proportion of H3K4me3-marked histones (H3K4me3$^+$), while enhancers have a higher proportion of H3K4me1 marked histones (H3K4me1$^+$). We identified promoter candidates as H3K4me3$^+$ regions, and retained those that overlapped a known (Pruitt et al., 2007) or reconstructed transcription start sites as identified from RNA-Seq data ((Guttman et al., 2010); Figure 2A, Figure S2 Methods). Notably, ~75% of the identified promoters were bound by at least one of the TFs. To define enhancers, we identified candidates containing H3K4me1$^+$ and retained those that were also bound by at least one TF (See for example the Il1a loci in Figure 2A; Methods). Altogether, we identified 38,439 enhancers and 11,505 promoters.

Consistent with previous observations (Ghisletti et al., 2010), we found that different chromatin marks exhibit different dynamics during stimulation (Figure S2C–I). For example H3K4me3 is remarkably stable during the first 2 hours of LPS response. The few exceptions

are in ~30 loci which are lowly expressed pre-stimulation and become strongly induced after stimulation (top 95% of induction). Conversely, H3K27Ac is more variable and tends to change in correlation with PolII binding (r=0.66 for H3K27Ac vs r=0.49 for H3K4me3). These chromatin marks are significantly less dynamic than most TFs (Figure S2C–I).

Global properties of TF binding maps

Taking all temporal reads together to obtain a "compressed" dataset, we identified significant binding events (peaks) for each TF (Guttman et al., 2010) (Methods). The vast majority (82%) of high scoring TF peaks fall within the promoter regions or the enhancer regions defined above (p<10^{-20}). The binding landscape is consistent with the known specificities of TFs (Methods, Table S5 and Figure S2J). Using *de-novo* motif discovery (Bailey and Elkan, 1994) across the high-scoring bound sites, we identified the known motifs for 20 (80%) of the TFs (Gupta et al., 2007), as well as novel motifs for E2f4, Ets2 and Ahr (12%). The highest scoring motif ($E < e^{-100}$) found for the TF E2f4 is the cell cycle genes homology region (CHR), a previously identified regulatory element found adjacent to a handful of cell cycle genes, which appears in tandem to an E2f canonical motif (Lange-zu Dohna et al., 2000).

The TFs vary in both number and location of binding events. Some TFs (PU.1 and Cebpb) bind >30,000 sites, while others (such as Hif1a) bind <1000 (Figure 2B), consistent with ChIP data for the same factors from other studies (Barish et al., 2010; Ghisletti et al., 2010; Heinz et al., 2010). Notably, ~70% of the identified peaks fall in close proximity (500bp) to a peak of either PU.1 or Cebpb (p<10^{-10}; Table S2). Different factors exhibit substantially different localization preferences with some favoring enhancers while others tend to bind in promoters or in less canonical regions (Figure 2). For example, the runt domain 1 factor Runx1 binds many targets at their 3′ UTR regions (Figure S3). Further analysis showed that Runx1 binding at the 3′ end tends to be stronger and more dynamic in comparison to promoter binding, and that the 3′ end target genes are more strongly expressed and have a stronger enrichment for an anti-inflammatory function. Examining genes that are down regulated upon Runx1 knock down in primary DC activated with LPS (Amit et al., 2009), we find a significant enrichment for inflammatory genes (p=0.003, hypergeometric) that are bound at their 3′ end. Taken together, these results suggest that Runx1 may have a different function when binding the 3′ end of genes as compared to promoter bound regions.

Co-binding of TFs in regulatory regions supports a Cis-regulatory organization

Associating each binding site with its associated regulatory region (promoter or enhancer) resulted in 184,805 high confidence interactions (Methods). Similar to recent reports (Zinzen et al., 2009), the resulting network suggests that TFs tend to bind in cis-Regulatory Modules (CRMs; Figure 3A; Table S2 and Figure S4A,B) occupied by multiple other factors (1.5 fold enrichment over a random model, p<10^{-10}; Supplementary text). Two notable factors, PU.1 and Cebpb tend to occupy most regions bound by all other factors but also bind many regions devoid of binding of the TFs we surveyed (>10% of their bound regions have no other factor binding, a 3-fold enrichment; p<10^{-10}; Figure S4C). PU.1 and Cebpb bound regions are also highly enriched in motifs of other TFs we did not survey (e.g. Klf, Myc, and Hlf; p < 10^{-10}) suggesting that PU.1 and Cebpb may co-bind with additional TFs at these sites (Ghisletti et al., 2010). Moreover, we find that ~8% of the regions are occupied by a larger number of TF than expected by chance. These regions, termed HOT regions (Gerstein et al., 2010; Negre et al., 2011; Roy et al., 2010), are defined to have 8 or more bound TFs (3.5-fold enrichment; Methods and Figure S4B).

TFs interact with one another in a combinatorial fashion to control different gene programs either by forming complexes that together bind DNA (Junion et al., 2012) or by

independently binding DNA regions (Arnosti and Kulkarni, 2005). We searched for co-occurring pairs of TFs, while excluding HOT regions, which can confound discovery of such interactions (Gerstein et al., 2010; Negre et al., 2011; Roy et al., 2010) (Figure 3, Methods). As expected, our results recapitulate well-known homotypic transcriptional complexes. For example, Rela co-occurs with other Nfkb family members (Relb, Nfkb1, cRel,(Smale, 2012)), Stat1 co-occurs with Stat2 and Irf1 co-occurs with Irf2. We also find novel heterotypic interactions such as, RelA-Runx1 and E2f4-Ets2 that warrant further exploration. Interestingly, the E2f4-Ets2 complex is enriched in cell-cycle genes that are dynamically repressed after stimulation ($p<10^{-3}$; Methods) (Table S3).

TFs range from primarily static to primarily dynamic binders

The TFs vary substantially in the extent of dynamic changes in their binding during the response. The Ifit locus, a robust anti-viral response cluster provides an illustrative example (Figure 4A). While PU.1 is bound at the same level in both un-stimulated and stimulated cells (Figure 4A, top inset), Stat1 binds only during the late stages of LPS response (Figure 4A, bottom inset). Globally only ~10% of the PU.1 binding sites are associated with substantial (>3-fold) changes post-stimulation, as opposed to ~90% of the Stat1 binding sites (Figure 4B, methods). Overall, 58,075 (31%) TF binding events are "dynamic" (Figure 4B, methods, and Figure S4D). In the following sections we analyze how temporal changes in the TF binding profiles correlate with the expression levels of their target genes.

Transcriptional induction potential is established prior to stimuli by a specific set of TFs

To study the functional impact of TF binding, we associated *cis*-regulatory regions with their target genes and generated a temporal TF-gene regulatory network containing 79,797 TF-gene interactions (Figure 4C,D, Methods). Overall, we find that genes bound by few TFs (<5) are enriched for basic cellular processes ($p<10^{-5}$), while genes targeted by many TFs (>15) are enriched for inflammatory response pathways ($p<10^{-7}$; Figure 4D, Table S3). The targets of individual TFs are also enriched for specific functional classes (Table S4). For example, E2f4 binding is enriched for cell cycle genes ($p<10^{-10}$); Nfkb binding is enriched for inflammatory response genes ($p<10^{-10}$); and Stat TF binding is enriched for anti-viral response genes ($p<10^{-10}$; Figure S5, Table S4).

To explore the relationship between binding dynamics and expression patterns we used temporal gene expression data using RNA-Seq for 5 different time-points (0, 1, 2, 4, 6 hours) following LPS stimulation. We divided the 4,993 genes that responded to LPS stimulation (2-fold change compared to the un-stimulated state, Methods) into five clusters (Figure 5A, Table S6, Figure S5A and Methods): The ~1,300 induced genes constituted three clusters: immediate early induced genes whose expression peaks before the first hour (293 genes), intermediate induced genes with peak expression prior to the second hour (227 genes), and late induced genes whose expression peaks after two hours (808 genes). Over 3,500 repressed genes comprised two additional clusters, genes that are gradually repressed and those that are rapidly repressed.

Genes in the LPS-induced clusters are bound by more TFs **prior** to the stimulus than non-induced genes ($p<10^{-10}$, Supplementary text). Furthermore, some of the factors (*e.g.*, Junb, Atf3, Irf4) are specifically enriched at the promoters or enhancers of these induced genes even *prior* to exposure to stimulus ($p<10^{-3}$, Figure 5A, S5A,B; Methods). In contrast, PU.1 and Cebpb bind a larger number of genes in the pre-stimulated state, but are not enriched for LPS-induced genes. These results suggest that transcriptional induction potential is established prior to stimulation via preferential binding of a selective set of TFs to inducible genes.

TF binding correlates with transcription dynamics

We next compared TF dynamics and gene expression following stimulation, finding multiple cases in which the timing of gain or loss of TF binding at genes in the induced clusters significantly precedes or coincides with the timing of transcriptional induction ($p<10^{-3}$; Figure S5C,D; Methods). We therefore further sub-clustered the genes within each expression profile by the similarity of their dynamic binding profiles, resulting in 19 clusters, each representing a unique combination of expression and binding profiles (Figure 5A, Methods, Table S3 and Figure S5E).

The 19 binding/expression clusters uncover different regulatory programs activated by innate immune DCs challenged with LPS. For instance, the late induced gene cluster is partitioned into two sub-groups. Late induced cluster II is strongly associated with late binding of Stat1 and Stat2 (Figure 5A,B, $p<10^{-3}$; Methods), and consists of highly expressed genes (average RPKM 250) that are enriched in interferon signaling and other anti-viral pathways ($p<10^{-10}$). In contrast, late induced cluster I is only weakly bound by the Stat factors, genes in this cluster have lower absolute expression levels (average RPKM 100) and are enriched mainly in leukocyte proliferation pathways and also in lowly expressed anti-viral genes ($p<10^{-5}$ and $p<10^{-10}$ respectively; Table S3). This partition suggests two different regulatory modes of late LPS gene activation: a high expression Stat-bound anti-viral response arm (Figure 5A,B), and a Stat-independent response arm, which orchestrates a second wave of inflammatory response genes (*e.g.*, CD86 that plays a critical role in T cell activation and survival (Sharpe and Freeman, 2002)).

Immediate early genes play a critical role in rapid response to changes in the environment, yet their mode of regulation is not fully understood (Amit et al., 2007; Hargreaves et al., 2009; Ramirez-Carrozzi et al., 2009; Weake and Workman, 2010). The immediate early genes are partitioned into three clusters, each associated with a distinct binding profile and enriched for genes from different pathways (Figure 5A). Immediate early cluster I is defined by strong binding of Rela and Egr1 during the first hour of stimulation, has a relatively low maximal expression (average RPKM 50) and is enriched for transcription factor genes, including Egr1, Egr2 and Egr3. In contrast, immediate early cluster II (Figure 5C) consists of highly expressed genes (average RPKM 300) that are targeted by a large number of TFs, many of which bind their targets prior to stimulation, and are enriched for inflammatory response genes (both TFs and cytokines, *e.g.*, Nfkbiz, Tnfaip3, Junb, Klf6 and TNF, $p<10^{-5}$; Figure S5E and Table S3). The low conservation together with the high degree of redundancy observed on immediate early genes (Figure S6, Supplementary text) suggests regulation via a 'billboard' or collective model rather than an enhanceosome model (Arnosti and Kulkarni, 2005). In this model, the billboard/collective is pre-assembled prior to stimuli and recruits, possibly without great specificity, many different factors on relatively non-conserved and weak binding sites to achieve high expression levels.

While induced genes are generally associated with gain of binding post-stimulation ($p<10^{-10}$), repressed clusters are enriched for loss of TF binding or for no binding gain ($p<10^{-10}$, Supplementary text). For instance, repressed cluster III (Figure 5A) is strongly enriched in cell cycle genes (*e.g.* Cdk1) and is primarily associated with static binding of the cell-cycle related factor E2f4 and Ets2 while it is depleted of binding of Junb, Irf4 and Atf3 which bind most of the induced genes. In another example, the histone gene locus is bound by Nfkb and E2f family members in the basal state, followed by loss of Nfkb factors immediately post-stimulation (Figure S5F). Together this suggests that genes that are not bound by priming factors pre-stimulation (Junb, Atf3 and Irf4) are more prone to repression following stimulation. A second alternative is that circuits involved in repression, like recruitment of the Smart/Ncor complex by Bcl6 (Barish et al., 2010), may be less profiled in

our study. We conclude that dynamic binding maps specify distinct regulatory programs and provide information on both timing and amplitude of gene expression.

A layered architecture of the TF network

The temporal structure of the TF network is consistent with a model of hierarchical organization and temporal dependencies between the different TFs where some TFs are bound prior to or concomitantly with other TFs. Such "layered architecture" of regulation has been described previously where Pioneer factors bind compacted chromatin, initiate chromatin remodeling during differentiation, and enable subsequent binding of non-Pioneers factors (Bossard and Zaret, 1998; Cirillo et al., 2002; Lupien et al., 2008).

To analyze the patterns of binding dependencies between the different TFs, we constructed a hierarchy graph (Figure 6A), where an edge is directed from factor A to factor B if factor A binds at least 30% of the regions bound by factor B at the same or earlier time. The graph reveals a clear organization that supports and extends the basic distinction between pioneers and non-pioneers. Not surprisingly, the **top-most tier** consists of the two factors in our set (PU.1 and Cebpb) previously described as pioneers (Ghisletti et al., 2010; Heinz et al., 2010). A **second tier** consists of three TFs (Junb, Irf4, Atf3), which bind pre-stimulation at LPS induced genes that later become associated with more specific and dynamic factors. Interestingly, in macrophages AP-1 binding motifs are also enriched at enhancers of LPS induced genes bound by the Pioneer factor PU.1 (Ghisletti et al., 2010). Our results suggest that Junb and Atf3 may be the AP-1 components at these sites. At the **bottom tier** we find factors that are more dynamic and control more specific sets of genes that have common biological functions. For instance, the Stat TFs target the late induced anti viral genes, while the Nfkb factors Rel, Relb and Nfkb1 target the inflammatory program.

To better characterize the TFs in the hierarchy we consolidated the various binding properties discussed above: (**1**) number of bound regions, (**2**) ratio of enhancer to promoter binding, (**3**) percent of dynamic binding events, (**4**) fraction of regions bound in isolation, (**5**) fraction of all DNA motifs in the genome bound by the factor, (**6**) Conservation of binding sites (see Supplementary text) (**7**) number of outgoing edges in the hierarchy, and (**8**) number of incoming edges in the hierarchy. Using Principal Component Analysis (Figure 6B) we found that the Pioneer factors, PU.1 and Cebpb clearly separate from all other factors. Both Cebpb and PU.1 are abundantly bound already in un-stimulated cells and cover the majority of sites bound by other TFs, but are also found in "isolated" sites with no binding by any of the analyzed TF. Furthermore, the binding of Cebpb and PU.1 is relatively static during the response, comparable to the histone marks and Ctcf (Figure 4B, Figure S2C–I). The remaining factors form at least two additional sub-groups. Factors in one group (Figure 6B green) bind many genes, but rarely bind in isolation (average 5% alone), have a larger proportion of dynamic binding events (36% vs. 12%) compared to the pioneers, and form an intermediate layer in the network, between the pioneers and the non-pioneer factors (Figure 6A). The remaining factors (Figure 6B red) tend to bind fewer genes, are mostly dynamic, tend to preferentially bind promoters, and are located lower in the hierarchy.

The factor classes are also distinguished by their effect on gene expression in a manner consistent with a 'layered' hierarchical organization. Pioneer binding correlates to a lesser degree with gene induction levels than factors in other tiers. Binding of second tier factors in the un-stimulated state correlates with the potential for induction (Figure S5A,B), but has lower enrichment for specific functional categories (Table S4). The remaining factors tend to bind a smaller number of regions from specific functional categories (e.g. Stat1 with anti-viral genes, E2f4 with cell cycle genes, Runx1 with Inflammatory genes) and dynamically coincide with the induction of genes post-stimulation (Figure 5, Figure S5C,D).

DISCUSSION

Mammalian genomes can give rise to hundreds of cell types and numerous transcriptional programs; this variety is largely encoded in TF-DNA networks, which are only partially understood. Our results indicate that the response of DCs to a pathogenic stimulus is encoded by a multilayered TF network that has at least three major layers (Figure 6): Pioneer factors potentiate binding by opening previously inaccessible sites (Bossard and Zaret, 1998; Cirillo et al., 2002; Heinz et al., 2010; Lupien et al., 2008). These new elements are occupied in a relatively static manner by second tier of TFs (e.g. Junb) that prime the response and set the basal expression levels of thousands of genes, and thus term them "Primer" factors. The final tier consists of TFs that bind subsets of genes, often in a very dynamic fashion, and usually at genes of a shared biological process (Smale, 2012).

The layer architecture we propose helps explain how the cell's expression potential is set during lineage commitment: while Pioneer factors initiate chromatin remodeling, Primer factors may serve as beacons, which upon stimulation direct other TFs or post-translation modifying enzymes to the appropriate genomic sites, a role previously suggested for pioneer factors such as Cebpb, PU.1, E2a and Ebf (Cirillo et al., 2002; Heinz et al., 2010).

Future work will be required to elucidate the exact mechanisms and nuclear complexes that these different classes of factors associate with to execute their diverse functions. For instance, in several cases we observe a Primer factor from one homotypic family joined or replaced by another factor from the same family (e.g. Egr1-Egr2, Irf members and several AP-1 factors) this may suggest that a partial role of the priming factors is to maintain the binding site or serve as a docking point for the dynamic partners from the same family. This proposed model may generalize to other transcriptional responses in different cell types (Mullen et al., 2011; Trompouki et al., 2011).

Our understanding of mammalian regulatory circuits is currently limited by technical constraints such as differences in the efficiency of antibodies or TF-DNA crosslinking. To overcome these limitations it will be important to generate reference-binding maps using tagged TFs, to directly benchmark antibody efficiency. The resulting inventory of ChIP antibodies and tagged TF libraries will enable the exploration of differences in TF physical networks under different conditions, cell types, or individuals in a population, and provide insights into the mammalian regulatory code and the role of specific *cis*-binding elements in disease (Kasowski et al., 2010). Such efforts will likely extend our proposed layered organization to other cellular states, and may enable efficient engineering of cellular identities by controlling the expression and timing of different regulatory layers.

Experimental Procedures

HT-ChIP

20 million DC were used for each ChIP experiment. Cells were fixed for 10 min with 1% formaldehyde, quenched with glycine and washed with ice-cold PBS and pellets where flash frozen in liquid nitrogen. Cross-linked DC where thawed on ice and resuspended in RIPA lysis buffer supplemented with protease inhibitor. Cells were lysed for 10 min on ice and the chromatin was sheared. The sonicated cell lysate was cleared by centrifugation and mixed with 75 ul of protein G magnetic dynabeads (Invitrogen) coupled to target antibody in 96 well plates and incubated over night at 4 degrees. Using 96 well magnets unbound cell lysate was removed and samples was washed 5 times with cold RIPA, twice with high salt RIPA, twice with LiCl buffer, twice with TE, and then eluted in 50 ul of elution buffer. The eluate was reverse crosslinked at 65C for 4 hours and then treated sequentially with 2ul of RNaseA for 30 min and 2.5 ul of Proteinase K for two hours. Solid-phase reversible

immobilization (SPRI) cleanup steps were performed in 96 well plates using the Bravo liquid handling platform (Agilent) using a modified version of (Fisher et al., 2011). 120ul SPRI beads were added to the reverse-crosslinked samples mixed and incubated for 2 minutes. Supernatant were separated from the beads using a 96-well magnet for 4 minutes. Beads were washed twice on the magnet with 70% ethanol and then air dried for 4 minutes. The DNA was eluted in 40 ul EB buffer. For the remainder of the library construction process (DNA end-repair, A-base addition, adaptor ligation and enrichment) a general SPRI cleanup involves addition of buffer containing 20% PEG and 2.5 M NaCl to the DNA reaction products (without moving the sample from the original well position). All enzymatic steps are carried out using enzymes from New England Biolabs. More-detailed description of the methods is provided in the Supplemental Experimental Procedures and http://www.weizmann.ac.il/immunology/AmitLab/data-and-method/HT-ChIP/.

Antibody quality control, Nanostring probe design and Enrichment validation

We designed ~4 probes targeting regulatory regions of ~200 genes centered at the TSS and complemented this set with two probes tiling of any significant PolII peak or K4me3 peak that lied within the gene body or any significant K4me3 peak that lied within 30Kb of the TSS of the genes we targeted. The final probeset consisted of 786 probes. See Experimental Procedures for more information.

Dendritic cell isolation, culture, and LPS stimulation

To obtain sufficient number of cells, we implemented a modified version of the DCs isolation used in (Lutz et al., 1999). See Experimental Procedures for more detailed information

RNA extraction and RNA-Seq library preparation

Total RNA was extracted with QIAzol reagent following the miRNeasy kit's procedure (Qiagen), and sample quality was tested on a 2100 Bioanalyzer (Agilent). We prepared the RNA-A+-Seq libraries using the 'dUTP second strand (strand specific) protocol as described in (Levine et al 2010). Libraries where sequenced using the Illumina Genome Analyzer (GAII), two lanes for each sample, corresponding to 45 million paired-end reads/sample on average.

Western Blot and antibody validation

Nuclear extracts from mouse bone marrow dendritic cells (DC) were prepared by using NE-PER nuclear and cytoplasmic extraction reagents (Thermo scientific, USA). 20ug of the nuclear proteins were separated by SDS-PAGE and transferred to PVDF membrane. Membranes were probed with antibodies and visualized by ECL, according to the instructions of the manufacturer.

Sequencing and read alignments

ChIP libraries were indexed, pooled and sequenced on Illumina HiSeq-2000 sequencers at the Broad Institute sequencing center. Reads were aligned to the reference mouse genome NCBI37, using BWA (Li and Durbin, 2009) version 0.5.7. RNA sequencing reads were aligned to the mouse reference genome (NCBI 37, MM9) using the TopHat aligner, version 1.1.4.(Trapnell et al., 2009) See supplementary Text more information.

Peak calling

We implemented our contiguous segmentation algorithm, described in (Guttman et al., 2009) as part of the Scripture package (available from http://www.broadinstitute.org/

software/scripture/) and used it to call, score and filter peaks for both chromatin and TF libraries. See supplementary text for more information.

Transcriptome annotation and quantification (RNA-Seq)

Top-Hat alignments were processed by Scripture (Guttman et al., 2010) to obtain significantly expressed transcripts for each time course. Only multi-exonic transcripts were retained. Quantification was used using the constituent model ((Garber et al., 2011) And Supplementary Text).

Motif analysis

We performed both de-novo motif discovery and known motif matching using the MEME-ChIP pipeline (http://meme.nbcr.net/meme4_6_1/memechip-intro.html).

Defining TF-region and TF-gene associations

The binding value of a TF in a region is the sum of enrichment scores over all the peaks that pass the detection cutoff during at least one time point. Gain or loss of binding are defined when there is at least 3-fold change in the binding value compared to the basal state (at t=0). We associate a gene with a gain (loss) event if at least 50% of its enhancers or 50% its promoters are associated with gain (loss). The association of regulatory regions with genes is described in the supplementary text.

A random model for binding complexity

We compared the observed TF complexities (Fig 4a) to a random model under which the complexity of a region is proportional to its length (Supplementary text). We use this analysis to define the cutoff for HOT regions as the minimal complexity value ($x>2$) for which the observed frequency is higher by at least two fold than the random one. The selected cutoff was $x=8$ (Fig S8).

Clustering

We employ a two-step k-means clustering process: first the genes were clustered by their temporal expression profiles, then each cluster is partitioned using the TF binding data. We used a randomization test in order to evaluate the dependency between the expression and binding data, as captured by the cluster analysis. To this end, we compare the distribution of cluster sizes obtained with the original data to that obtained from randomized instances, shuffling the binding data while retaining the expression levels and the number of binding TF per-gene (Kolmogorov-Smirnov $p<10^{-10}$).

Evaluating enrichment of TF binding in gene sets

We evaluate the enrichment of TF binding in a set of genes (Figure. 5b,c) using a hypergeometric score. In order to control for the general tendency of TF to be associated with highly expressed genes (Figure S17), we shuffle the binding data while maintaining the correlation between the number of bound TF and expression magnitude. We then compute an empirical p-value by comparing the randomized scores to the original ones. To get more specific results we also exclude genes that are associated with HOT regions.

Supplementary Material

Refer to Web version on PubMed Central for supplementary material.

Acknowledgments

References

Amit I, Citri A, Shay T, Lu Y, Katz M, Zhang F, Tarcic G, Siwak D, Lahad J, Jacob-Hirsch J, et al. A module of negative feedback regulators defines growth factor signaling. Nat Genet. 2007; 39:503–512. [PubMed: 17322878]

Amit I, Garber M, Chevrier N, Leite AP, Donner Y, Eisenhaure T, Guttman M, Grenier JK, Li W, Zuk O, et al. Unbiased reconstruction of a mammalian transcriptional network mediating pathogen responses. Science. 2009; 326:257–263. [PubMed: 19729616]

Arnosti DN, Kulkarni MM. Transcriptional enhancers: Intelligent enhanceosomes or flexible billboards? Journal of cellular biochemistry. 2005; 94:890–898. [PubMed: 15696541]

Bailey TL, Elkan C. Fitting a mixture model by expectation maximization to discover motifs in biopolymers. Proc Int Conf Intell Syst Mol Biol. 1994; 2:28–36. [PubMed: 7584402]

Barish GD, Yu RT, Karunasiri M, Ocampo CB, Dixon J, Benner C, Dent AL, Tangirala RK, Evans RM. Bcl-6 and NF-kappaB cistromes mediate opposing regulation of the innate immune response. Genes & development. 2010; 24:2760–2765. [PubMed: 21106671]

Barski A, Cuddapah S, Cui K, Roh TY, Schones DE, Wang Z, Wei G, Chepelev I, Zhao K. High-resolution profiling of histone methylations in the human genome. Cell. 2007; 129:823–837. [PubMed: 17512414]

Bossard P, Zaret KS. GATA transcription factors as potentiators of gut endoderm differentiation. Development. 1998; 125:4909–4917. [PubMed: 9811575]

Capaldi AP, Kaplan T, Liu Y, Habib N, Regev A, Friedman N, O'Shea EK. Structure and function of a transcriptional network activated by the MAPK Hog1. Nat Genet. 2008; 40:1300–1306. [PubMed: 18931682]

Cirillo LA, Lin FR, Cuesta I, Friedman D, Jarnik M, Zaret KS. Opening of compacted chromatin by early developmental transcription factors HNF3 (FoxA) and GATA-4. Mol Cell. 2002; 9:279–289. [PubMed: 11864602]

Davidson EH. Emerging properties of animal gene regulatory networks. Nature. 2010; 468:911–920. [PubMed: 21164479]

Fisher S, Barry A, Abreu J, Minie B, Nolan J, Delorey TM, Young G, Fennell TJ, Allen A, Ambrogio L, et al. A scalable, fully automated process for construction of sequence-ready human exome targeted capture libraries. Genome biology. 2011; 12:R1. [PubMed: 21205303]

Garber M, Grabherr MG, Guttman M, Trapnell C. Computational methods for transcriptome annotation and quantification using RNA-seq. Nat Methods. 2011; 8:469–477. [PubMed: 21623353]

Gerstein MB, Lu ZJ, Van Nostrand EL, Cheng C, Arshinoff BI, Liu T, Yip KY, Robilotto R, Rechtsteiner A, Ikegami K, et al. Integrative analysis of the Caenorhabditis elegans genome by the modENCODE project. Science. 2010; 330:1775–1787. [PubMed: 21177976]

Ghisletti S, Barozzi I, Mietton F, Polletti S, De Santa F, Venturini E, Gregory L, Lonie L, Chew A, Wei CL, et al. Identification and characterization of enhancers controlling the inflammatory gene expression program in macrophages. Immunity. 2010; 32:317–328. [PubMed: 20206554]

Graf T, Enver T. Forcing cells to change lineages. Nature. 2009; 462:587–594. [PubMed: 19956253]

Gupta S, Stamatoyannopoulos JA, Bailey TL, Noble WS. Quantifying similarity between motifs. Genome biology. 2007; 8:R24. [PubMed: 17324271]

Guttman M, Amit I, Garber M, French C, Lin MF, Feldser D, Huarte M, Zuk O, Carey BW, Cassady JP, et al. Chromatin signature reveals over a thousand highly conserved large non-coding RNAs in mammals. Nature. 2009; 458:223–227. [PubMed: 19182780]

Guttman M, Garber M, Levin JZ, Donaghey J, Robinson J, Adiconis X, Fan L, Koziol MJ, Gnirke A, Nusbaum C, et al. Ab initio reconstruction of cell type-specific transcriptomes in mouse reveals the conserved multi-exonic structure of lincRNAs. Nat Biotechnol. 2010; 28:503–510. [PubMed: 20436462]

Harbison CT, Gordon DB, Lee TI, Rinaldi NJ, Macisaac KD, Danford TW, Hannett NM, Tagne JB, Reynolds DB, Yoo J, et al. Transcriptional regulatory code of a eukaryotic genome. Nature. 2004; 431:99–104. [PubMed: 15343339]

Hargreaves DC, Horng T, Medzhitov R. Control of inducible gene expression by signal-dependent transcriptional elongation. Cell. 2009; 138:129–145. [PubMed: 19596240]

Heintzman ND, Ren B. Finding distal regulatory elements in the human genome. Current opinion in genetics & development. 2009; 19:541–549. [PubMed: 19854636]

Heinz S, Benner C, Spann N, Bertolino E, Lin YC, Laslo P, Cheng JX, Murre C, Singh H, Glass CK. Simple combinations of lineage-determining transcription factors prime cis-regulatory elements required for macrophage and B cell identities. Mol Cell. 2010; 38:576–589. [PubMed: 20513432]

Johnson DS, Mortazavi A, Myers RM, Wold B. Genome-wide mapping of in vivo protein-DNA interactions. Science. 2007; 316:1497–1502. [PubMed: 17540862]

Junion G, Spivakov M, Girardot C, Braun M, Gustafson EH, Birney E, Furlong EE. A transcription factor collective defines cardiac cell fate and reflects lineage history. Cell. 2012; 148:473–486. [PubMed: 22304916]

Kasowski M, Grubert F, Heffelfinger C, Hariharan M, Asabere A, Waszak SM, Habegger L, Rozowsky J, Shi M, Urban AE, et al. Variation in transcription factor binding among humans. Science. 2010; 328:232–235. [PubMed: 20299548]

Lange-zu Dohna C, Brandeis M, Berr F, Mossner J, Engeland K. A CDE/CHR tandem element regulates cell cycle-dependent repression of cyclin B2 transcription. FEBS Lett. 2000; 484:77–81. [PubMed: 11068036]

Laslo P, Spooner CJ, Warmflash A, Lancki DW, Lee HJ, Sciammas R, Gantner BN, Dinner AR, Singh H. Multilineage transcriptional priming and determination of alternate hematopoietic cell fates. Cell. 2006; 126:755–766. [PubMed: 16923394]

Li H, Durbin R. Fast and accurate short read alignment with Burrows-Wheeler transform. Bioinformatics. 2009; 25:1754–1760. [PubMed: 19451168]

Lupien M, Eeckhoute J, Meyer CA, Wang Q, Zhang Y, Li W, Carroll JS, Liu XS, Brown M. FoxA1 translates epigenetic signatures into enhancer-driven lineage-specific transcription. Cell. 2008; 132:958–970. [PubMed: 18358809]

Lutz MB, Kukutsch N, Ogilvie AL, Rossner S, Koch F, Romani N, Schuler G. An advanced culture method for generating large quantities of highly pure dendritic cells from mouse bone marrow. Journal of immunological methods. 1999; 223:77–92. [PubMed: 10037236]

Mikkelsen TS, Ku M, Jaffe DB, Issac B, Lieberman E, Giannoukos G, Alvarez P, Brockman W, Kim TK, Koche RP, et al. Genome-wide maps of chromatin state in pluripotent and lineage-committed cells. Nature. 2007; 448:553–560. [PubMed: 17603471]

Mullen AC, Orlando DA, Newman JJ, Loven J, Kumar RM, Bilodeau S, Reddy J, Guenther MG, DeKoter RP, Young RA. Master transcription factors determine cell-type-specific responses to TGF-beta signaling. Cell. 2011; 147:565–576. [PubMed: 22036565]

Negre N, Brown CD, Ma L, Bristow CA, Miller SW, Wagner U, Kheradpour P, Eaton ML, Loriaux P, Sealfon R, et al. A cis-regulatory map of the Drosophila genome. Nature. 2011; 471:527–531. [PubMed: 21430782]

Pruitt KD, Tatusova T, Maglott DR. NCBI reference sequences (RefSeq): a curated non-redundant sequence database of genomes, transcripts and proteins. Nucleic acids research. 2007; 35:D61–65. [PubMed: 17130148]

Rabani M, Levin JZ, Fan L, Adiconis X, Raychowdhury R, Garber M, Gnirke A, Nusbaum C, Hacohen N, Friedman N, et al. Metabolic labeling of RNA uncovers principles of RNA production and degradation dynamics in mammalian cells. Nat Biotechnol. 2011; 29:436–442. [PubMed: 21516085]

Ram O, Goren A, Amit I, Shoresh N, Yosef N, Ernst J, Kellis M, Gymrek M, Issner R, Coyne M, et al. Combinatorial Patterning of Chromatin Regulators Uncovered by Genome-wide Location Analysis in Human Cells. Cell. 2011; 147:1628–1639. [PubMed: 22196736]

Ramirez-Carrozzi VR, Braas D, Bhatt DM, Cheng CS, Hong C, Doty KR, Black JC, Hoffmann A, Carey M, Smale ST. A unifying model for the selective regulation of inducible transcription by CpG islands and nucleosome remodeling. Cell. 2009; 138:114–128. [PubMed: 19596239]

Robinson JT, Thorvaldsdottir H, Winckler W, Guttman M, Lander ES, Getz G, Mesirov JP. Integrative genomics viewer. Nat Biotechnol. 2011; 29:24–26. [PubMed: 21221095]

Roy S, Ernst J, Kharchenko PV, Kheradpour P, Negre N, Eaton ML, Landolin JM, Bristow CA, Ma L, Lin MF, et al. Identification of functional elements and regulatory circuits by Drosophila modENCODE. Science. 2010; 330:1787–1797. [PubMed: 21177974]

Segal E, Shapira M, Regev A, Pe'er D, Botstein D, Koller D, Friedman N. Module networks: identifying regulatory modules and their condition-specific regulators from gene expression data. Nat Genet. 2003; 34:166–176. [PubMed: 12740579]

Sharpe AH, Freeman GJ. The B7-CD28 superfamily. Nature reviews Immunology. 2002; 2:116–126.

Smale ST. Dimer-specific regulatory mechanisms within the NF-kappaB family of transcription factors. Immunological reviews. 2012; 246:193–204. [PubMed: 22435556]

Struhl K. Gene regulation. A paradigm for precision. Science. 2001; 293:1054–1055. [PubMed: 11498564]

Thanos D, Maniatis T. The high mobility group protein HMG I(Y) is required for NF-kappa B-dependent virus induction of the human IFN-beta gene. Cell. 1992; 71:777–789. [PubMed: 1330326]

Trapnell C, Pachter L, Salzberg SL. TopHat: discovering splice junctions with RNA-Seq. Bioinformatics. 2009; 25:1105–1111. [PubMed: 19289445]

Trompouki E, Bowman TV, Lawton LN, Fan ZP, Wu DC, DiBiase A, Martin CS, Cech JN, Sessa AK, Leblanc JL, et al. Lineage regulators direct BMP and Wnt pathways to cell-specific programs during differentiation and regeneration. Cell. 2011; 147:577–589. [PubMed: 22036566]

Weake VM, Workman JL. Inducible gene expression: diverse regulatory mechanisms. Nature reviews Genetics. 2010; 11:426–437.

Zinzen RP, Girardot C, Gagneur J, Braun M, Furlong EE. Combinatorial binding predicts spatio-temporal cis-regulatory activity. Nature. 2009; 462:65–70. [PubMed: 19890324]
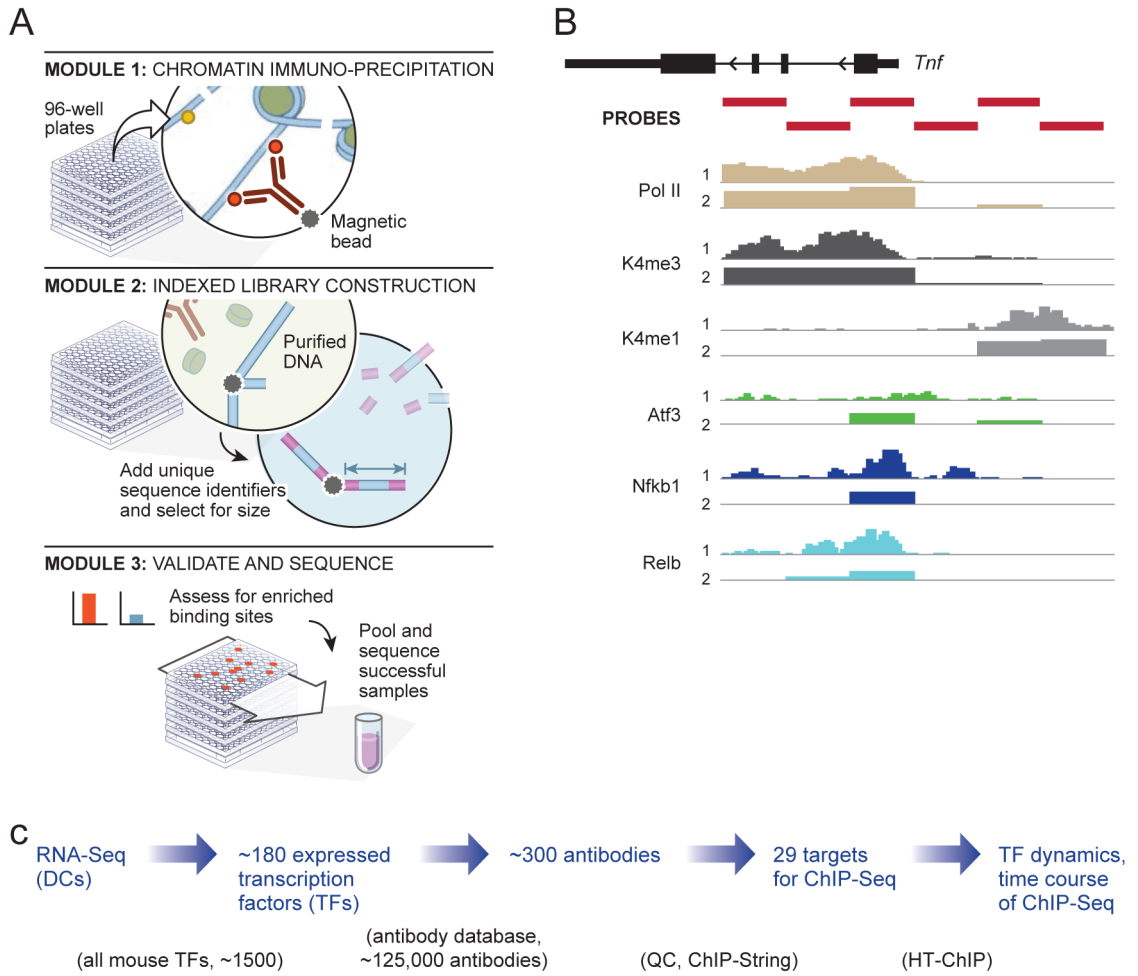
Figure 1. High throughput Chromatin Immuno-precipitation (HT-ChIP) pipeline
A. Blueprint of the HT-ChIP pipeline **Top**, Protein-DNA fragments are precipitated using antibody coupled magnetic beads in 96-well plates. **Middle**. Precipitated DNA is purified using magnetic beads, indexed adapters are ligated and size selected to generate sequencing libraries. **Bottom**. Samples are validated using ChIP-String; successful samples are pooled and sequenced. **B.** ChIP-String validation. Nanostring probes (red) target selected active regulatory regions. Comparison of (a) ChIP-Seq (b) or ChIP-String for K4me1 (gray) K4me3 (dark grey), Pol-II (light brown) Relb, and Nfkb1 (variants of blue), and Atf3 (green) **C.** Strategy for *ab initio* TF-DNA binding maps. The strategy consists of four steps 1. Expression analysis using RNA-Seq (2) Selection of top expressed TFs (3) Screening for all potential ChIP-Seq antibodies (4) ChIP in appropriate time points all validated TF targets.
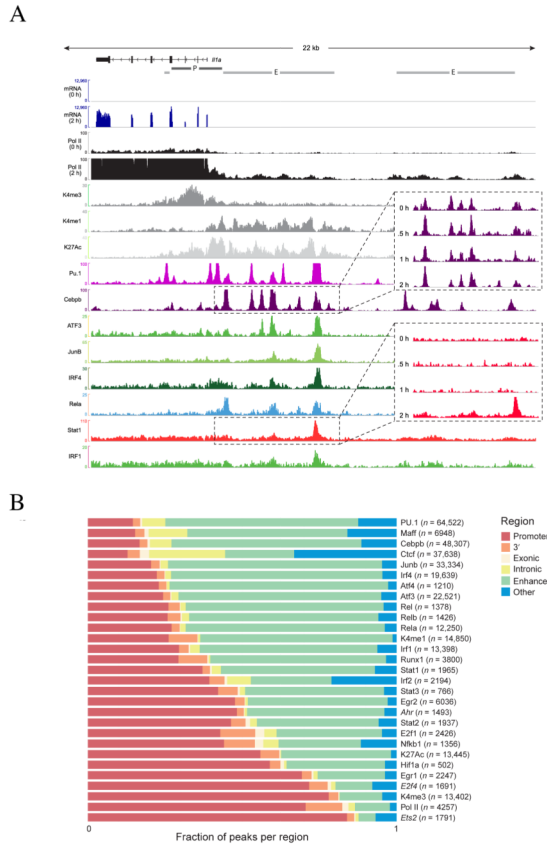
Figure 2. Epigenetic and transcription factor binding landscape
A. Representative Integrative Genomics Viewer (IGV) tracks, in the Il1a loci showing
RNA-Seq expression and "compressed" alignments for selected TFs and histone
modifications (Supplemental text). Enhancer and promoter calls (Methods) are shown on
top. Call-out boxes show time course data for selected factors. **B.** Distribution of the peaks
across promoter, 3′UTR, exonic, intronic, enhancer and unannotated, regions. Each bar
shows the fraction of peaks that overlap each region type. The total number of peaks is
shown in parenthesis. Factors in italics indicate that the motif shown is not the canonical
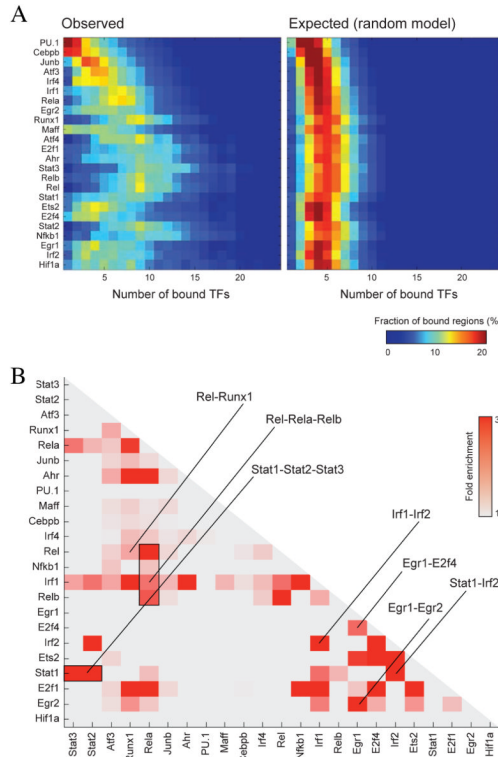binding motif for the factor.

Figure 3. Co-binding of TFs in regulatory regions

A. We define the *TF complexity* of a regulatory region as the number of TF bound to it (Roy et al., 2010). The heatmaps show for every TF a distribution of the complexities associated with its bound regions. The left heatmap shows the original data while the right heatmap is obtained from a random process in which the TF complexity of every region is proportional to its length (Methods). **B.** TF co-binding at similar regions. Significant TF pairs ($p<10^{-3}$, Methods) are color-coded by their respective fold enrichment. Selected overlaps are highlighted.
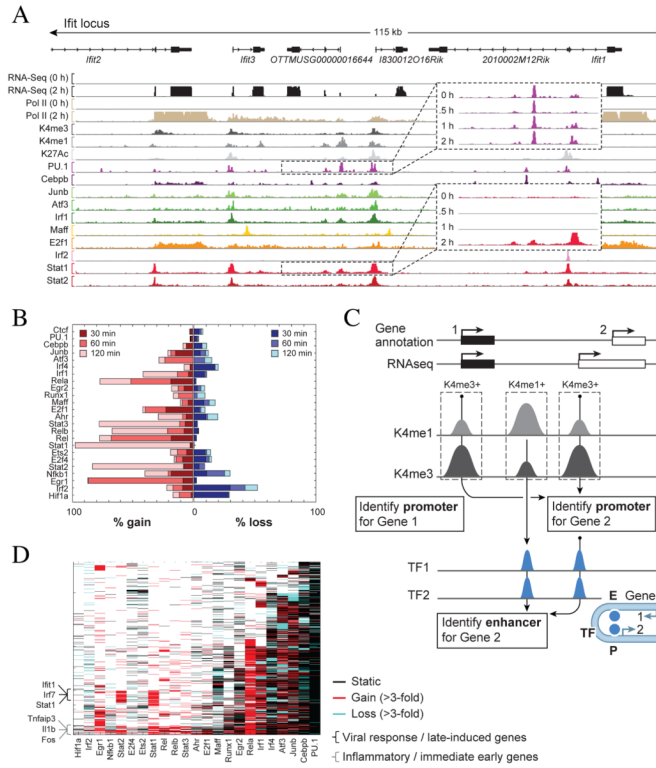
Figure 4. Dynamics of TF binding
A. Representative IGV tracks, in the Ifit locus showing RNA-Seq expression and
"compressed" alignments for selected TFs and histone modifications (Supplemental text).
Call-out boxes show time course data for an example of static binding (PU.1) and an
example of dynamic binding (Stat1). **B.** Bar plot showing the fraction of TF peaks gained
(>3 fold increase compared to the un-stimulated state; left plot) or lost (>3 fold decrease;
right plot) during the response to LPS. Each bar is subdivided and colored to represent the
fraction of peaks that are gained (lost) at each time point (Methods). **C.** A schematic
example of our enhancer and promoter annotation strategy and their association to genes.
Top: two cartoon genes (in black and white), gene 2 has a previously unannotated alternative
start site discovered through RNA-Seq. Middle: Promoters were defined as H3K4me3 rich
regions (H3K4me3[+]) that either overlap an existing annotation or a reconstructed transcript.
Enhancers were associated with TF-bound H3K4me1 rich regions (H3K4me1[+]). Bottom:
Both gene 1 and 2 are within 150kb away from the annotated enhancer, however, we
associate the enhancer with gene 2 since its promoter shares a common TF with the
enhancer. Bottom right: A cartoon model of looping between the annotated enhancer and the
promoter of gene 2 **D.** Binding of TF (x-axis) at regulatory elements of genes (y-axis); black
cells indicate no change in binding over time; red cells are increased binding and blue cells
are decreased binding (Methods). Genes were clustered into 8 groups based on their binding
profile (Table S3). On the left we indicate clusters that are enriched ($p<10^{-10}$) in anti-viral,
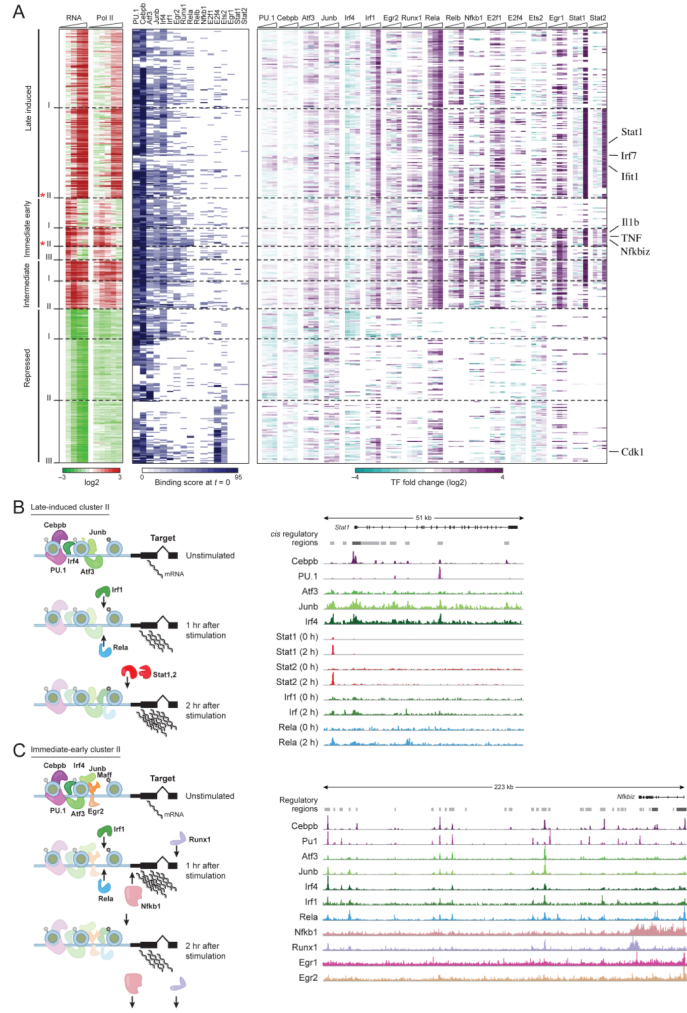inflamatory, early induced (induce within 1 hour), and late-induced genes (induced after 2
hours).

Figure 5. Associating TF binding dynamics with gene expression
A. Differentially expressed genes were clustered by expression (RNA-Seq) and TF binding. The heat map depicts all the induced clusters and 3 representative repressed clusters. The x-axis of the left heatmap shows fold change in RNA expression (RNA-Seq) for 4 time-points (1hr, 2hrs, 4hrs and 6hrs) post stimulation compared with the un-stimulated levels. Similarly, the second heatmap on the left shows fold changes in Pol-II enrichment for 5 time-points (15 min, 30 min, 60 min, 120 min and 240 min). The third heatmap displays binding enrichment scores at the un-stimulated state. The fourth heatmap shows fold changes of binding over time relative to the un-stimulated state. **B and C.** Left: Cartoon model depicting the transcriptional regulation of the late induced cluster II (B) and immediate early cluster II (C). Shown are TF with significant binding enrichment on genes in the cluster (Methods). Right: IGV tracks, showing the loci of representative genes: Stat1 (Late induced) and Nfkbiz (Immediate early cluster II).
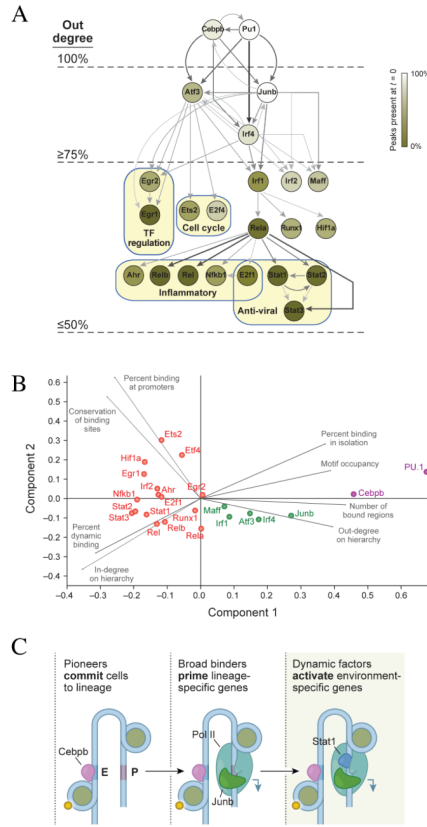
Figure 6. Diversity of binding properties suggests a layered TF architecture
A. The TF hierarchy graph. A directed edge goes from a TF X to a TF Y if X binds in at least 30% of the regions bound by Y at the same or earlier time. Edge color is determined by the coverage of X over Y (30–100%; see Table S8 for coverage values). The nodes are color coded according to the percentage of binding sites that were already bound pre-stimulation. For clarity of presentation we employed a pruning strategy (Methods) that removes direct links between nodes at the top of the hierarchy to nodes at the bottom of the hierarchy. Each connected component in the network (rooted at PU.1 or Cebpb) represents a unique combination of TF. The combinations in the trimmed network cover 78% of the TF-region binding data. The number of out-going edges in the non-pruned hierarchy graph (*out degree*) for nodes at different layers is provided on the left (presented values are the fraction of the maximum out degree). **B.** Principle Components Analysis was performed with several binding characteristics (Methods). The plot depicts the projections of the TFs and the loading of the different covariates for the first two principle components. **C.** Model depicting the layered TF network architecture: Pioneer factors initially bind and initiate remodeling of the epigenome, strong binders prime targets for expression and specific TFs control expression of smaller subsets of genes.